Recent changes in terrestrial water storage in the Upper Nile Basin: an evaluation of commonly used gridded GRACE products

Mohammad Shamsudduha[1, 2], Richard G. Taylor[2], Darren Jones[3], Laurent Longuevergne[4], Michael Owor[5] and Callist Tindimugaya[6]

[1]Institute for Risk and Disaster Reduction, University College London, London, UK
[2]Department of Geography, University College London, London, UK
[3]Centre for Geography, Environment and Society, University of Exeter, Exeter, UK
[4]CNRS – UMR 6118 Géosciences Rennes, Université de Rennes 1, Rennes, France
[5]Department of Geology & Petroleum Studies, Makerere University, Kampala, Uganda
[6]Directorate of Water Resources Management, Ministry of Water & Environment, Uganda

Correspondence to: M. Shamsudduha (m.shamsudduha@ucl.ac.uk)

Supplementary Material

Supplementary Table:

Table S1. Mean annual (2003–2012) amplitudes (first row) and variability (i.e., variance, cm^2) in in situ ΔTWS explained by individual signals (second row) such as various GRACE-derived ΔTWS, simulated ΔSMS, in situ ΔSWS and in situ ΔGWS in both LVB (120 cm^2) and LKB (24 cm^2) and the relative proportion of variability (third row) in in situ ΔTWS as explained by ΔSMS, ΔSWS and ΔGWS.

Lake Victoria Basin (LVB)					
GRACE Ensemble ΔTWS	GRGS ΔTWS	JPL-MASCON ΔTWS	ΔSMS	ΔSWS	ΔGWS
11.7 cm	20.6 cm	20.5 cm	7.9 cm	14.8 cm	4.4 cm
77%	91%	85%	59%	89%	32%
-	-	-	9.4%	88.6%	1.9%
Lake Kyoga Basin (LKB)					
8.4 cm	16.2 cm	16.4 cm	7.3 cm	3.8 cm	3.5 cm
55%	49%	53%	56%	51%	64%
-	-	-	55.9%	37.2%	6.9%

Supplementary Figures:

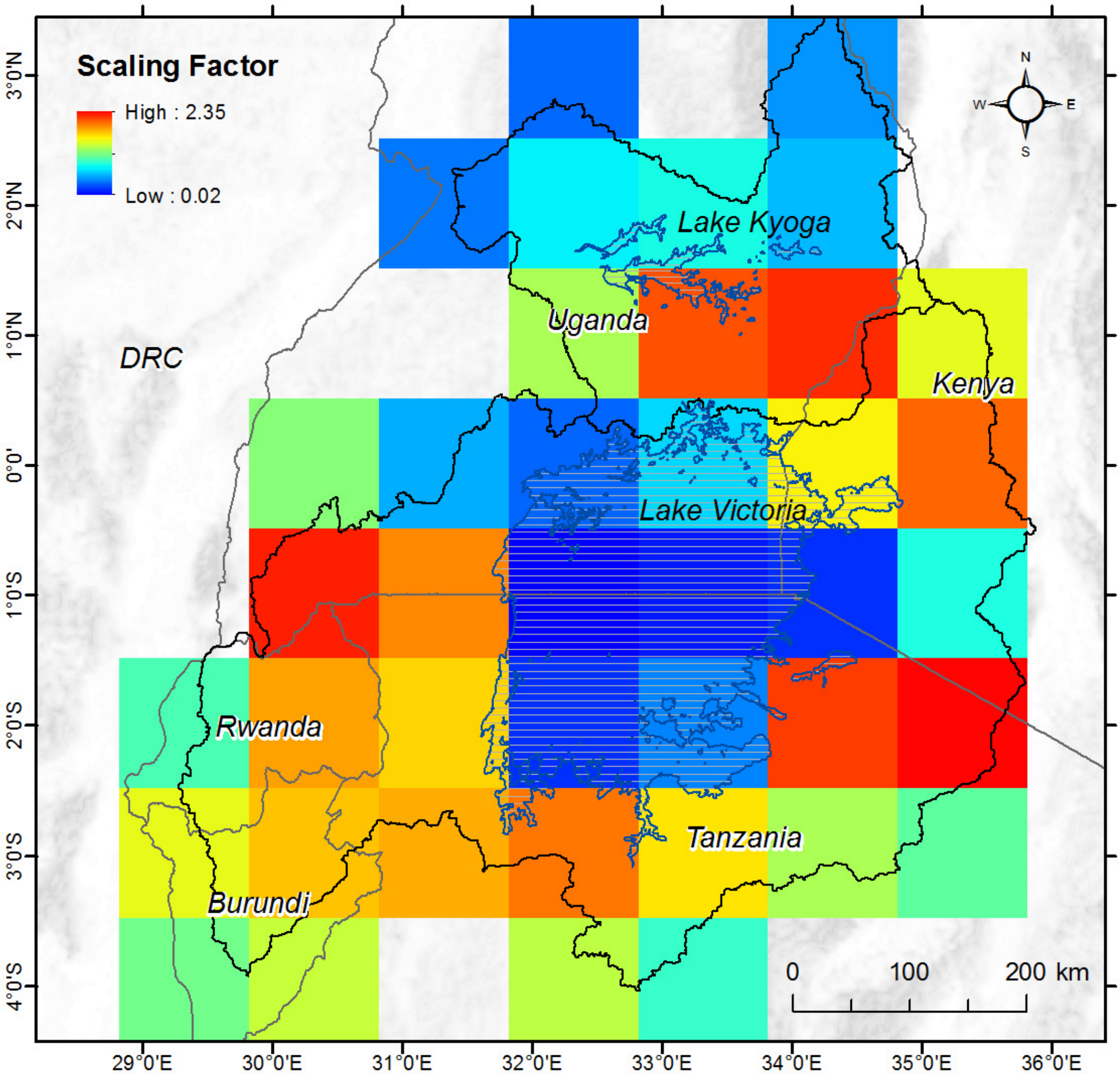

Figure S1. The general outline of Lake Victoria Basin (LVB) and Lake Kyoga Basin (LKB) within the Upper Nile Basin and the gridded scaling coefficients derived from CLM4.0 land surface model (Landerer and Swenson, 2012).

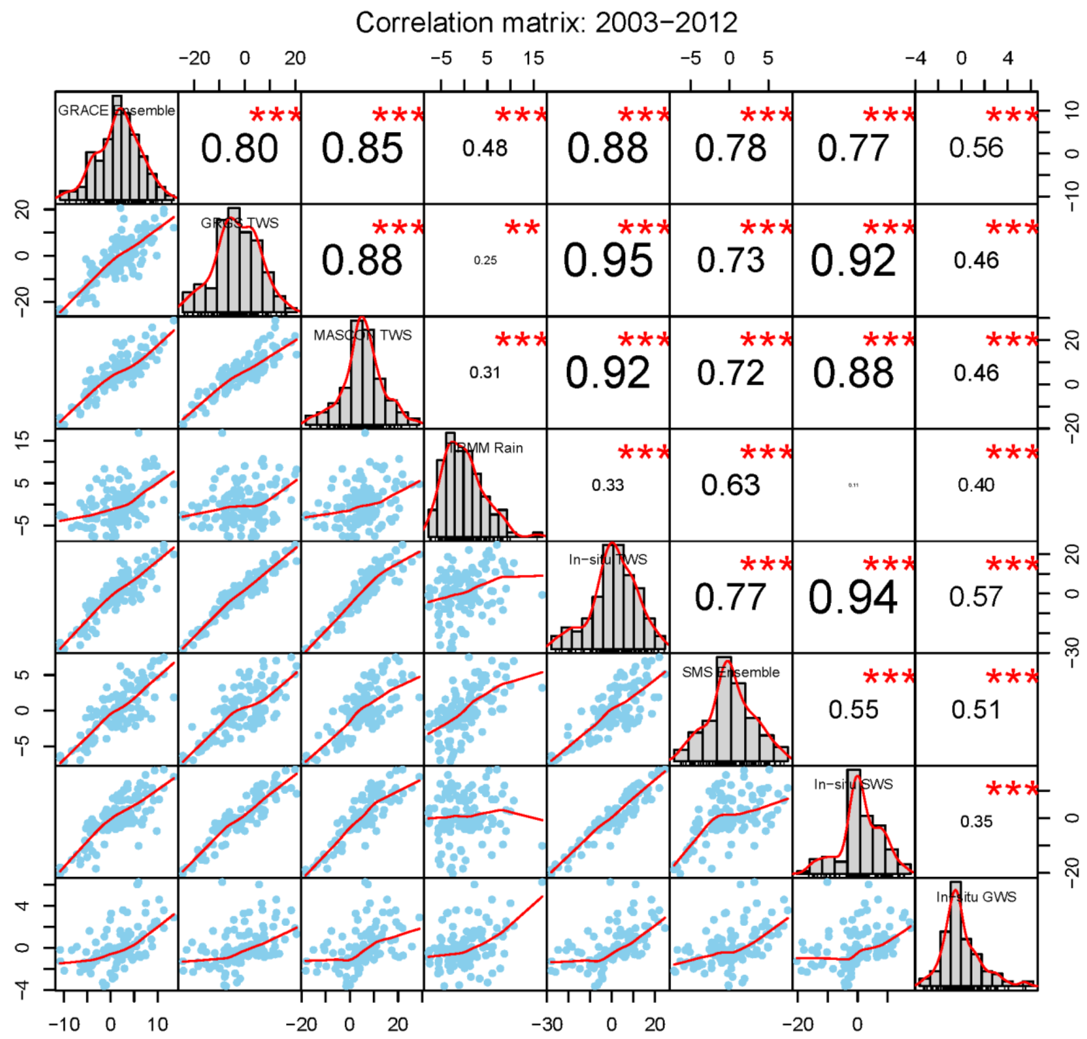

Figure S2. Pearson correlation coefficients among the time-series variables collated over the Lake Victoria Basin for the period of 2003 to 2012. Statistically significant correlated variables are marked with asterisks where the significance asterisks represent *p*-values < 0.05 (1 asterisk), <0.01 (2 asterisks) and <0.001 (3 asterisks). Histograms with kernel density overlays and bivariate scatterplots of variables are shown. The fitted curve lines in bivariate scatterplots represent locally-weighted polynomial regression (i.e., Lowess) lines.

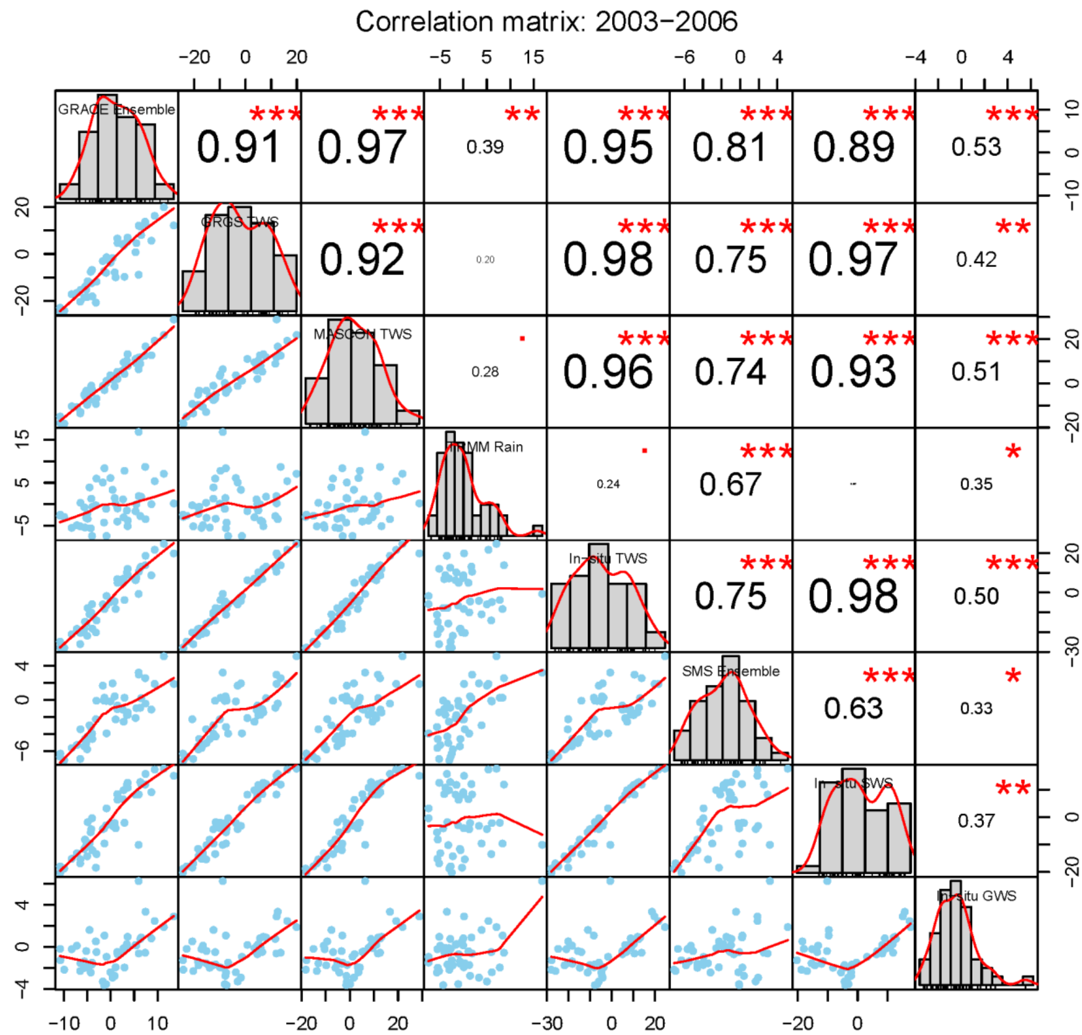

Figure S3. Pearson correlation coefficients among the time-series variables collated over the Lake Victoria Basin for the period of 2003 to 2006. Statistically significant correlated variables are marked with asterisks where the significance asterisks represent *p*-values < 0.05 (1 asterisk), <0.01 (2 asterisks) and <0.001 (3 asterisks). Histograms with kernel density overlays and bivariate scatterplots of variables are shown. The fitted curve lines in bivariate scatterplots represent locally-weighted polynomial regression (i.e., Lowess) lines.

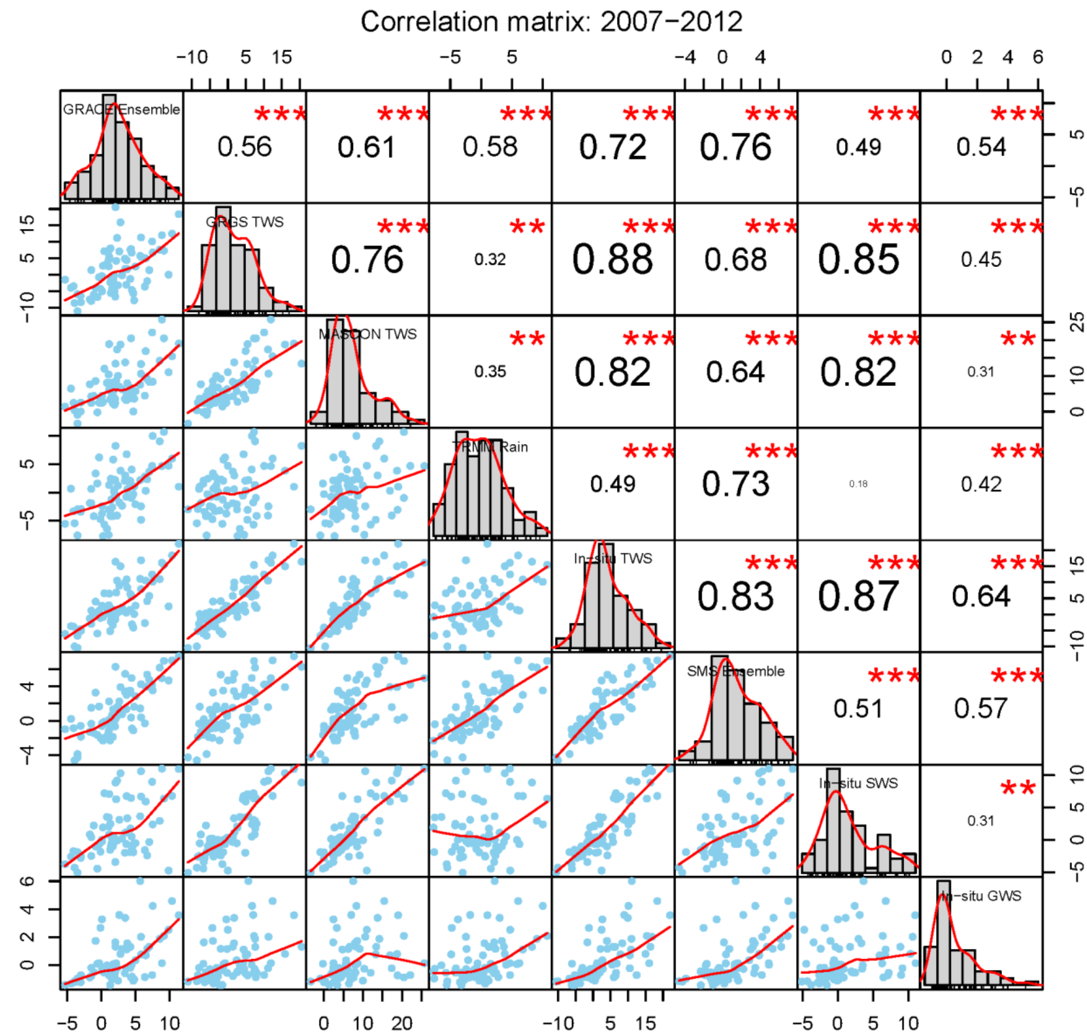

Figure S4. Pearson correlation coefficients among the time-series variables collated over the Lake Victoria Basin for the period of 2007 to 2012. Statistically significant correlated variables are marked with asterisks where the significance asterisks represent *p*-values < 0.05 (1 asterisk), <0.01 (2 asterisks) and <0.001 (3 asterisks). Histograms with kernel density overlays and bivariate scatterplots of variables are shown. The fitted curve lines in bivariate scatterplots represent locally-weighted polynomial regression (i.e., Lowess) lines.

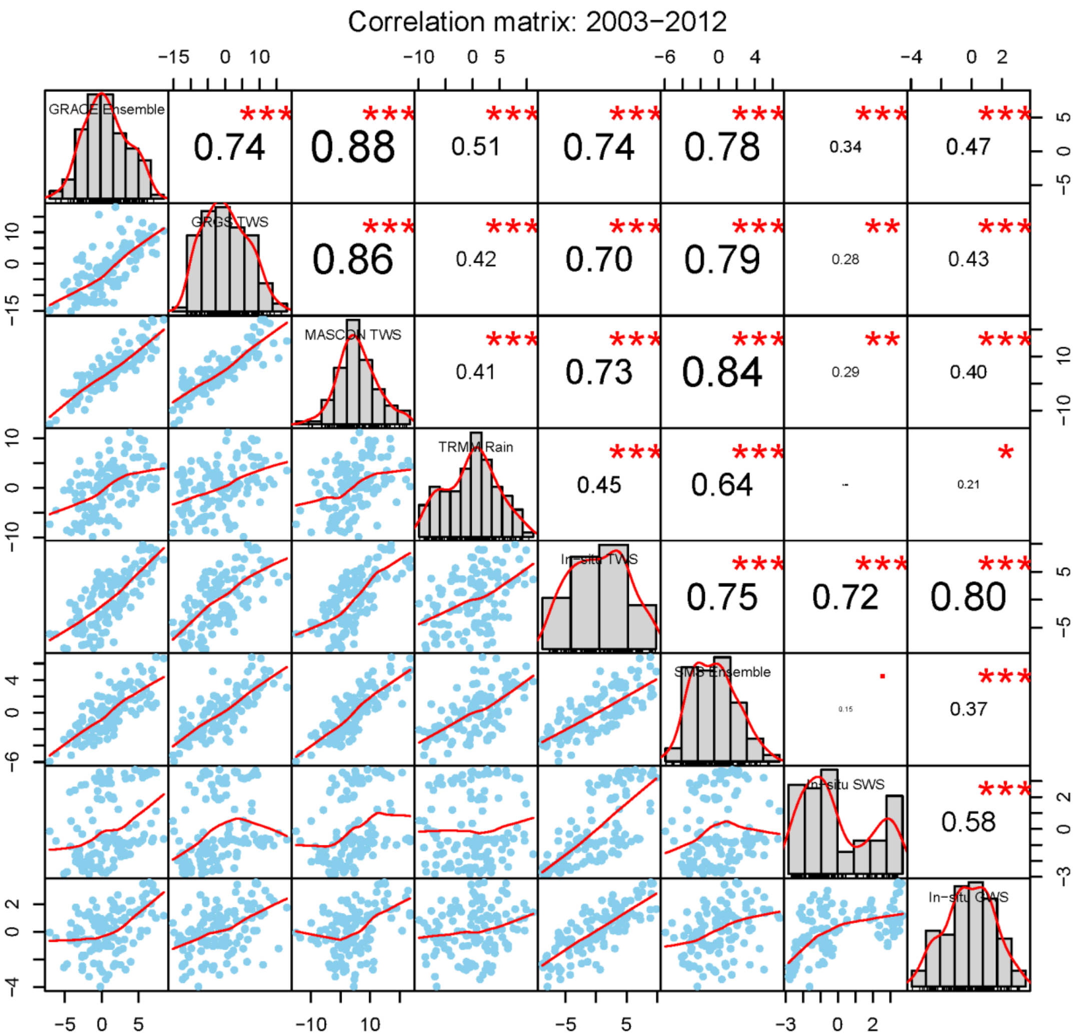

Figure S5. Pearson correlation coefficients among the time-series variables collated over the Victoria Nile Basin for the period of 2003 to 2012. Statistically significant correlated variables are marked with asterisks where the significance asterisks represent *p*-values < 0.05 (1 asterisk), <0.01 (2 asterisks) and <0.001 (3 asterisks). Histograms with kernel density overlays and bivariate scatterplots of variables are shown. The fitted curve lines in bivariate scatterplots represent locally-weighted polynomial regression (i.e., Lowess) lines.

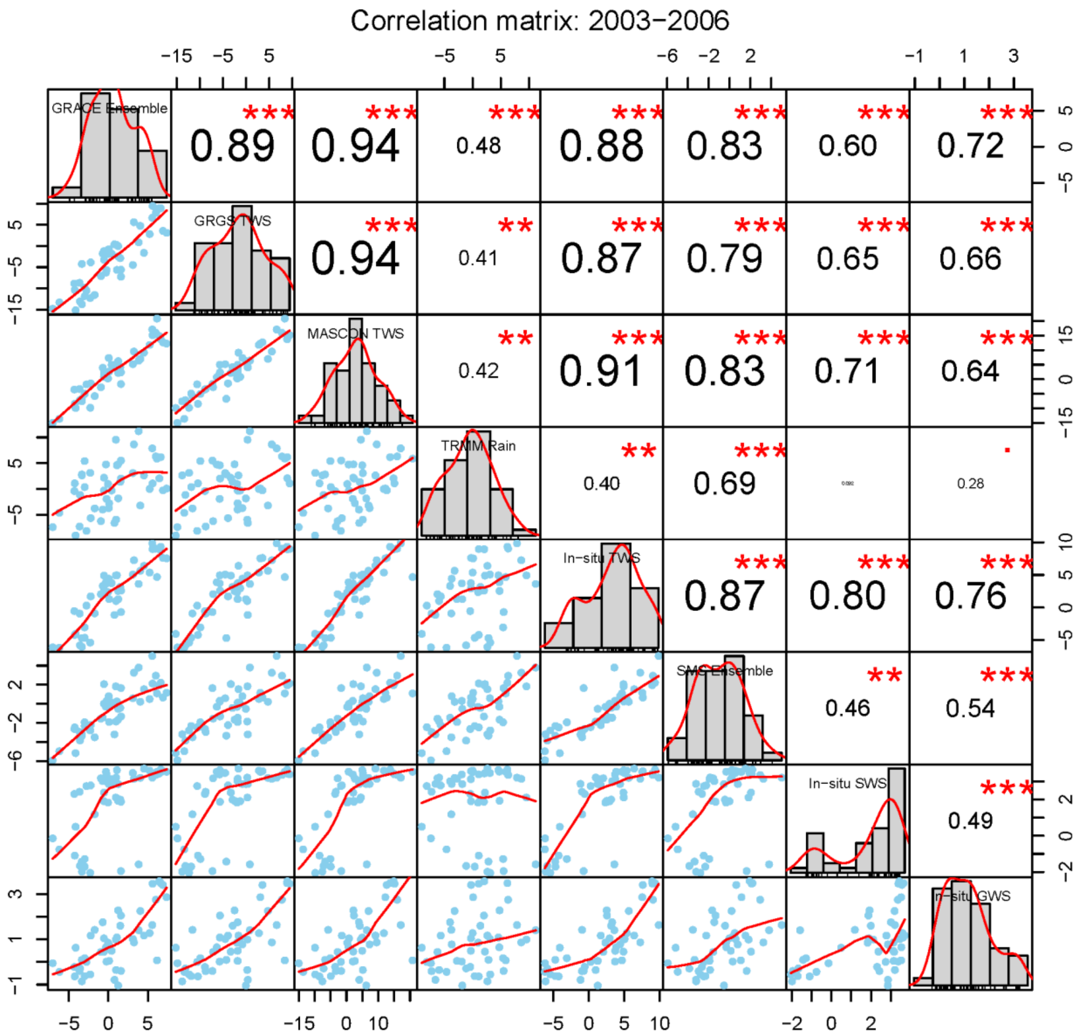

Figure S6. Pearson correlation coefficients among the time-series variables collated over the Victoria Nile Basin for the period of 2003 to 2006. Statistically significant correlated variables are marked with asterisks where the significance asterisks represent *p*-values < 0.05 (1 asterisk), <0.01 (2 asterisks) and <0.001 (3 asterisks). Histograms with kernel density overlays and bivariate scatterplots of variables are shown. The fitted curve lines in bivariate scatterplots represent locally-weighted polynomial regression (i.e., Lowess) lines.

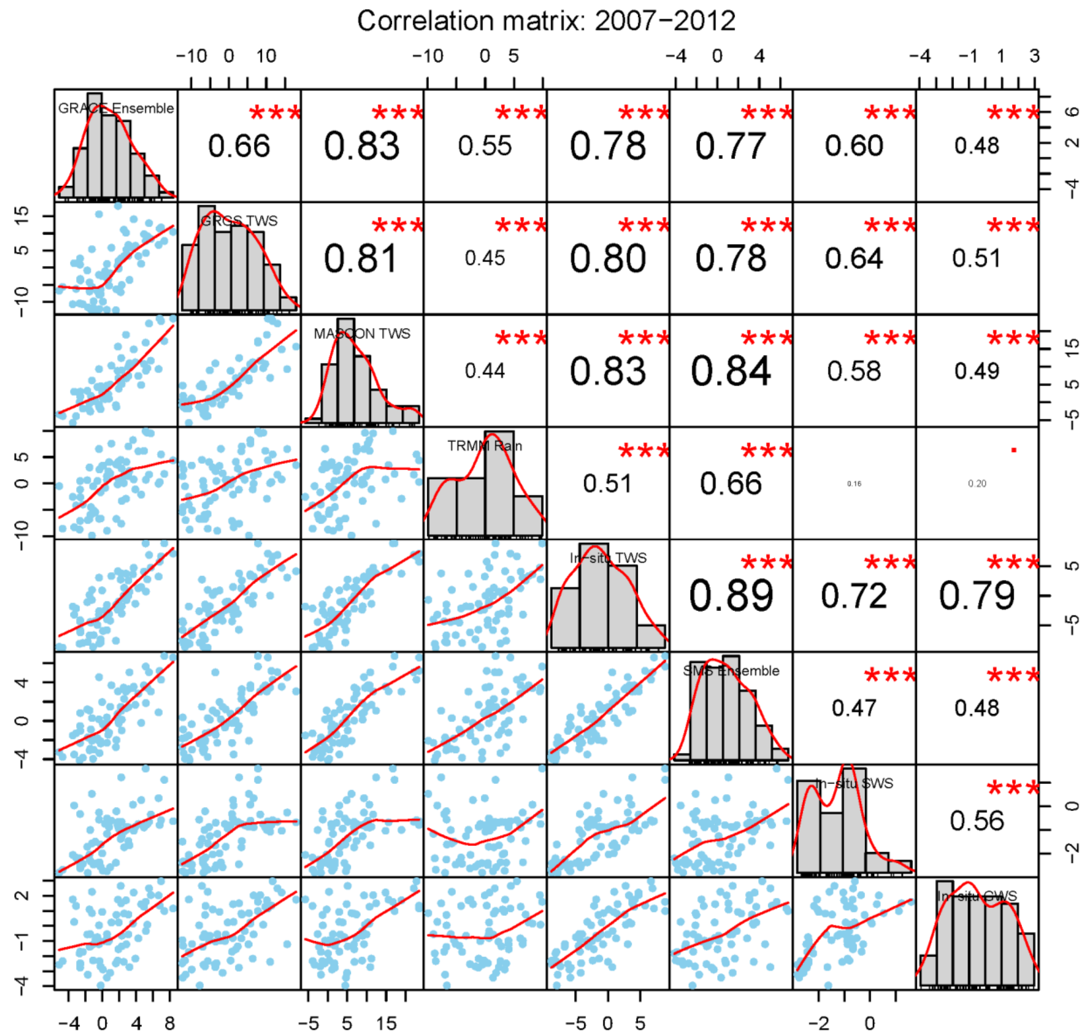

Figure S7. Pearson correlation coefficients among the time-series variables collated over the Victoria Nile Basin for the period of 2007 to 2012. Statistically significant correlated variables are marked with asterisks where the significance asterisks represent *p*-values < 0.05 (1 asterisk), <0.01 (2 asterisks) and <0.001 (3 asterisks). Histograms with kernel density overlays and bivariate scatterplots of variables are shown. The fitted curve lines in bivariate scatterplots represent locally-weighted polynomial regression (i.e., Lowess) lines.

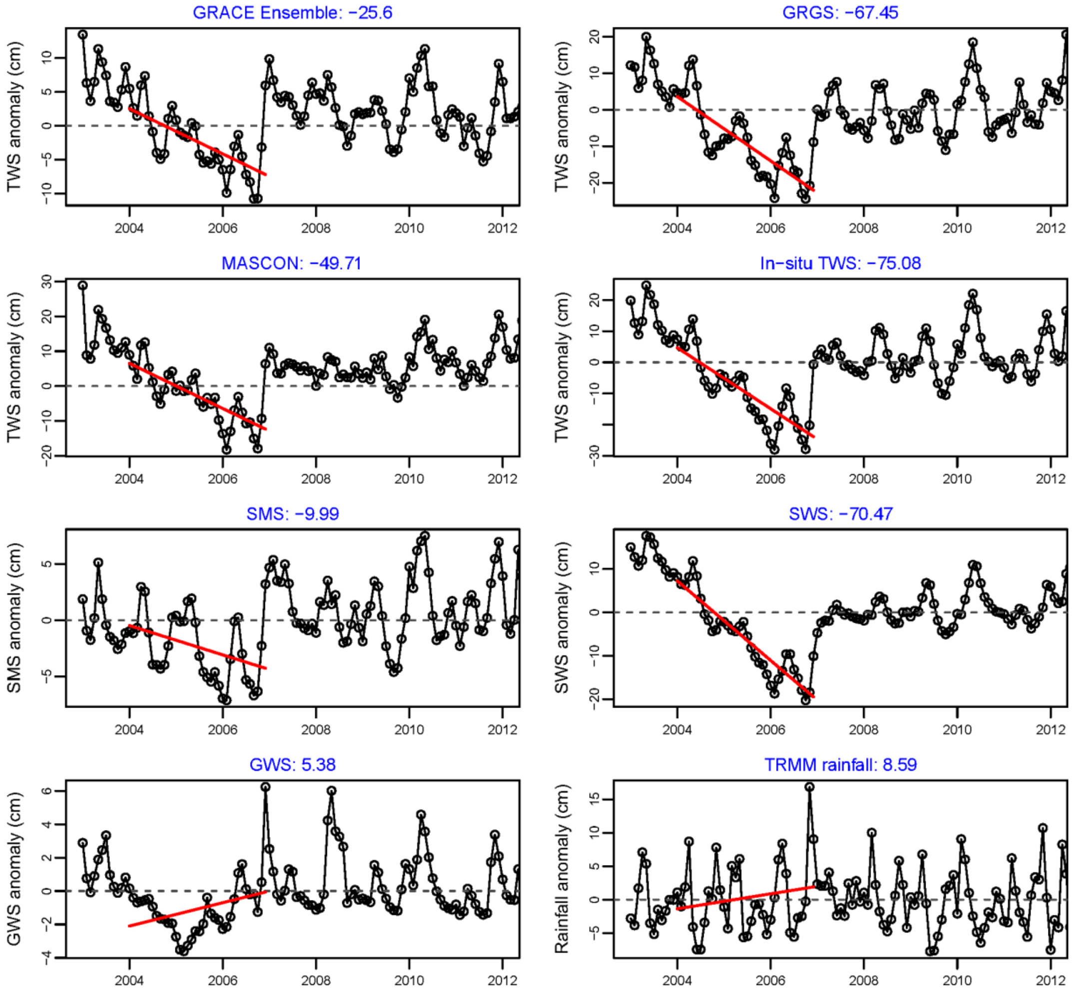

Figure S8. Time-series records of various GRACE ΔTWS signals, in-situ ΔTWS, in-situ ΔSWS, simulated ΔSMS and in-situ ΔGWS in LVB and linear trends (red line) for the period of 2004 to 2006. Figure (blue) on top of each panel indicates the estimated storage change in km^3.

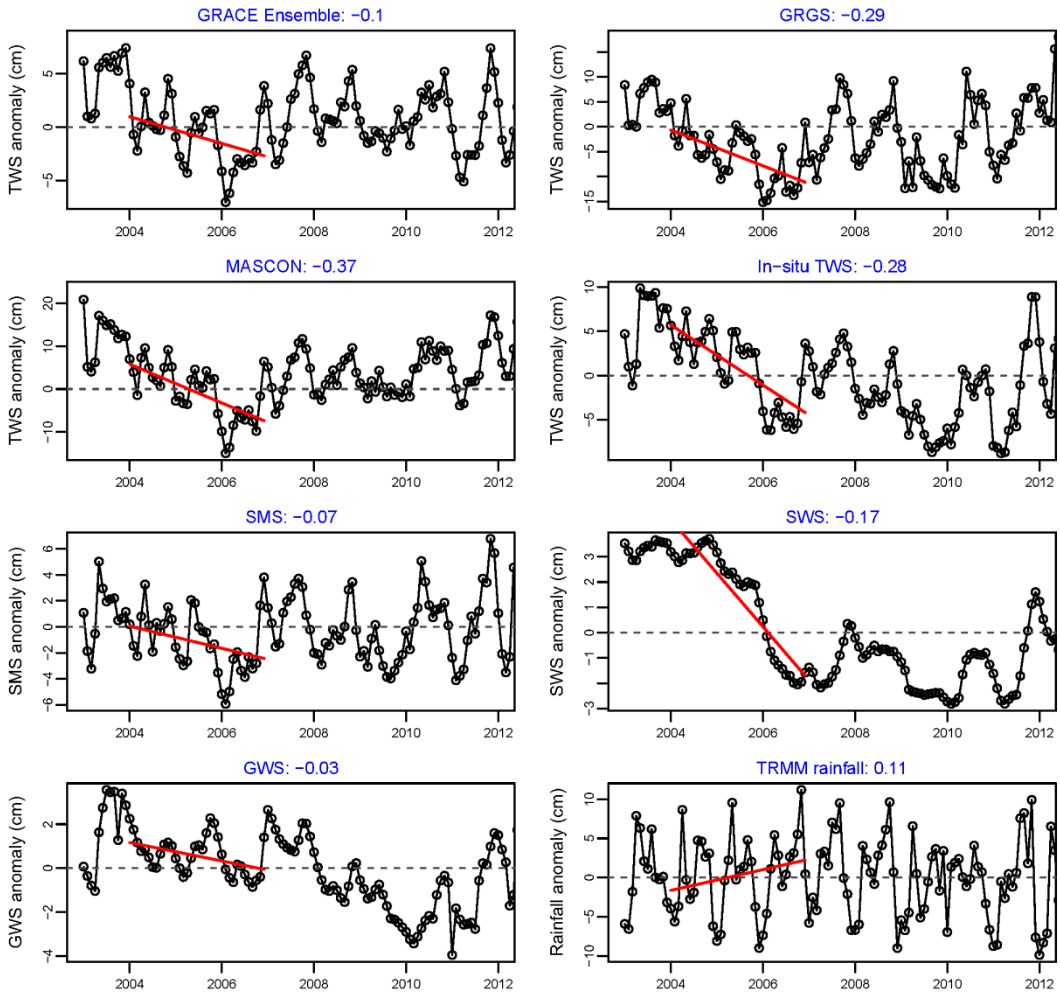

Figure S9. Time-series records of various GRACE ΔTWS signals, in-situ ΔTWS, in-situ ΔSWS, simulated ΔSMS and in-situ ΔGWS in VNB and linear trends (red line) for the period of 2004 to 2006. Figure (blue) on top of each panel indicates the estimated storage change in km^3.

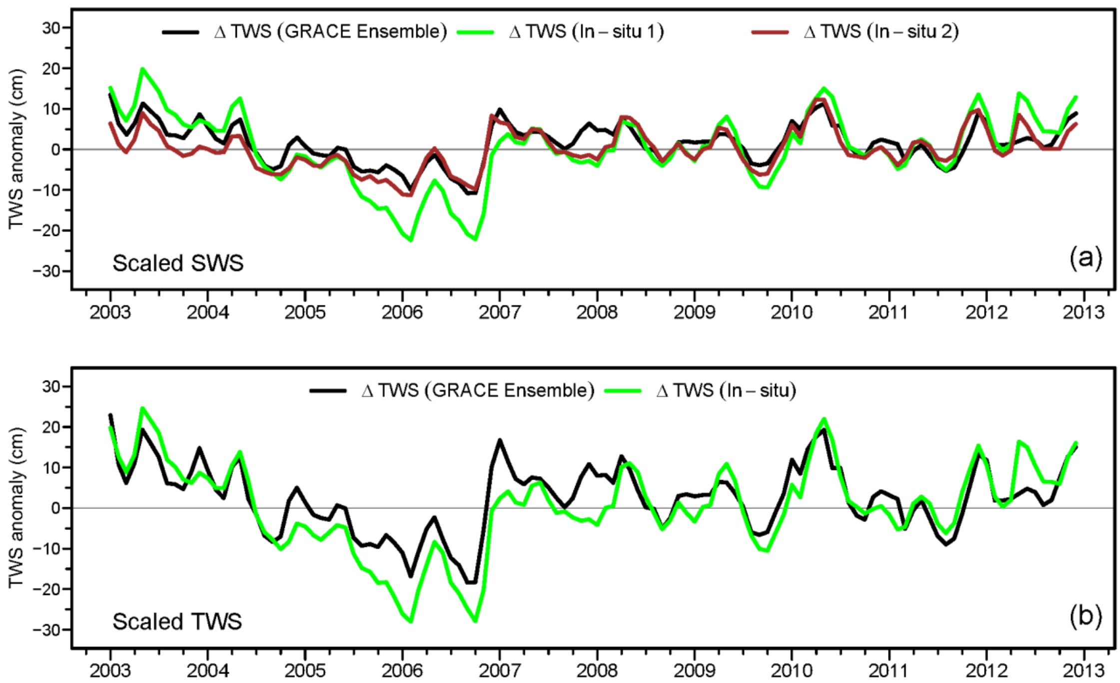

Figure S10. Results of scaling experiments on GRACE and in situ ΔTWS over LVB. Panel (a) shows the comparison between *GRCTellus* GRACE-derived ΔTWS and in situ ΔTWS where a scaled down (scaling factor of 0.77 in situ ΔTWS-1; scaling factor of 0.11 in situ ΔTWS-2) ΔSWS signal is applied; on bottom panel (b) shows comparison between *GRCTellus* GRACE-derived ΔTWS and in situ ΔTWS where the GRACE-ΔTWS signal is scaled up by a factor of 1.7 that shows the lowest RMSE of 5.76 cm.

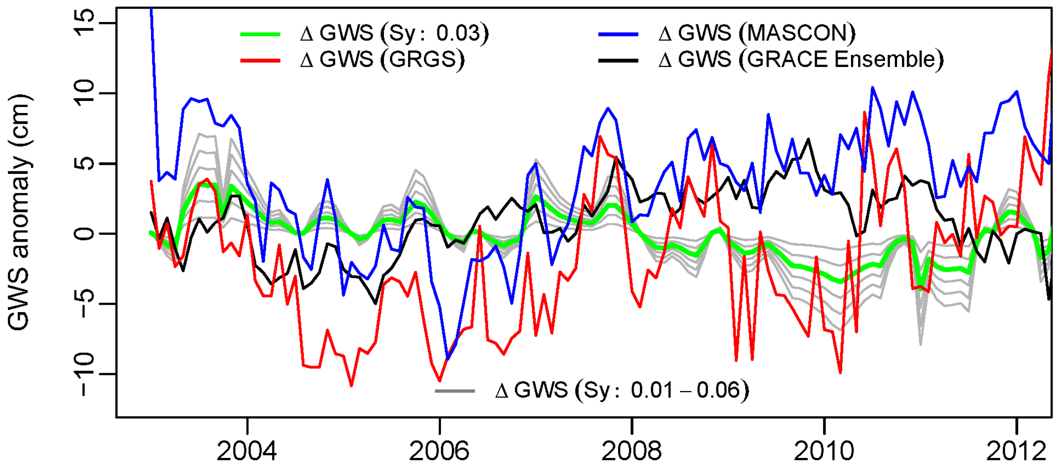

Figure S11. Estimates of in situ ΔGWS and GRACE-derived ΔGWS time-series records (2003–2012) in LKB show a substantial variations among themselves. Unlike LVB no scaling experiments were applied for LKB in the disaggregation of ΔGWS using *GRCTellus* (ensemble mean of CSR, GFZ, and JPL) and JPL-Mascons GRACE products.

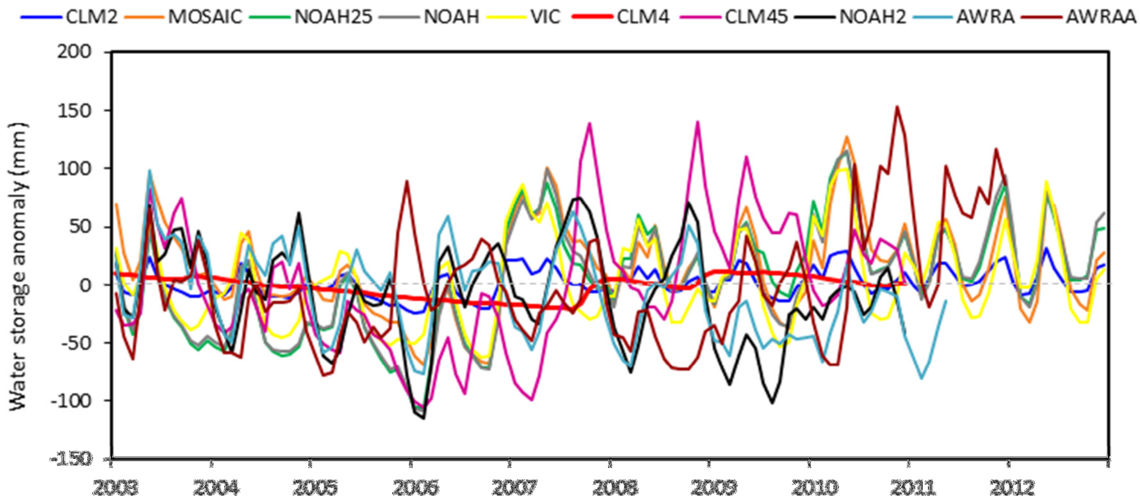

Figure S12. Simulated terrestrial water storage anomaly from 10 LSMs for the Lake Victoria Basin. Note that not all LSMs simulate groundwater storage; for example, latest versions of the Community Land Model (CLM4.0 and 4.5) simulate groundwater storage.